

Physical Separation Processes

Food technology has evolved from the practice of preserving products in very much the same form as they occur in nature to one where desirable components are separated and converted to other forms. Separation processes have been in use in the food industry for years, but sophistication in its use is a fairly recent occurrence. Current technology makes it possible to remove haze from wine and fruit juices or nectars, separate the proteins of cheese whey into fractions having different functional properties, separate foreign matter from whole or milled grains, and concentrate fruit juices without having to employ heat. Efficient separation processes have been instrumental in making economically viable the recovery of useful components from food processing wastes.

13.1 FILTRATION

Filtration is the process of passing a fluid containing suspended particles through a porous medium. The medium traps the suspended solids producing a clarified filtrate. Filtration is employed when the valuable component of the mixture is the filtrate. Examples are clarification of fruit juices and vegetable oil. If the suspended material is the valuable component (e.g., recovery of precipitated proteins from an extracting solution), and rapid removal of the suspending liquid cannot be carried out without the addition of a filter aid, other separation techniques must be used.

Surface filtration is a process where the filtrate passes across the thickness of a porous sheet while the suspended solids are retained on the surface of the sheet. A sheet with large pores has low resistance to flow therefore filtrate flow is rapid, however, small particles may pass through resulting in a cloudy filtrate. Surface filtration allows no cake accumulation. Flow stops when solids cover the pores. If the solids do not adhere to the filter surface, the filter may be regenerated by backwashing the surface. Filtration sterilization of beer using microporous filters is a form of surface filtration.

Depth filtration is a process where the filter medium is thick, and solids penetrate the depth of the filter. Eventually, solids block the pores and stop filtrate flow, or solids may break through the filter and contaminate the filtrate. Once filtrate flow stops or slows down considerably, the filter must be replaced. In depth filtration, particle retention may occur by electrostatic attraction in addition to the sieving effect. Thus, particles smaller than the pore size may be retained. Depth filters capable of electrostatic solids retention will be ideal for rapid filtration. Cartridge, fiber, and sand filters are forms of depth filtration. Depth filtration is not very effective when suspended solids concentration is very high.

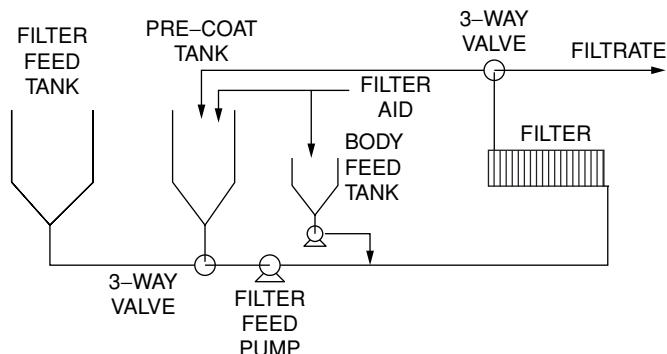


Figure 13.1 Diagram of filter system for filter aid filtration.

Filter aid filtration involves the use of agents that form a porous cake with the suspended solids. Filter aids used commercially are diatomaceous earth and perlite. Diatomaceous earth consists of skeletal remains of diatoms and is very porous. Perlite is milled and classified perlite rock, an expanded crystalline silicate. In filter aid filtration, the filter medium is a thin layer of cloth or wire screen that has little capacity for retention of the suspended solids and serves only to retain the filter aid. A layer of filter aid (0.5 to 1 kg/m^2 of filter surface) is precoated over the filter medium before the start of filtration. Filter aid, referred to as “body feed,” is continuously added to the suspension during filtration. As filtration proceeds, the filter aid and suspended solids are deposited as a filter cake, which increases in thickness with increasing filtrate volume. Body feed filter aid concentration is usually in the range of one to two times the suspended solids concentration. A body feed concentration must be used that will produce a cake with adequate porosity for filtrate flow. Inadequate body feed concentration of filter aid will result in rapid decrease in filtrate flow and consequently shorten filtration cycles. Figure 13.1 is a diagram of a filtration system for filter aid filtration. The system is designed to make it easy to change from precoat operation to body feed filtration operation with the switch of a 3-way valve. Some filters such as the vertical leaf filter can be backflushed to remove the filter cake. Some, like the plate and frame filter, are designed to be easily disassembled to remove the filter cake. The body feed may be a slurry of the filter aid that is metered into the filter feed, or the dry filter aid may be added using a proportional solids feeder into the filter feed tank. In continuous vacuum filters, precoating is done only once at the start of the operation. Body feed is added directly to the vacuum filter pan. Figure 13.2 is a diagram of the most common filters used for filter aid filtration. Figure 13.2A is a vertical leaf filter, Fig. 13.2B is a plate and frame filter, and Fig. 13.2C is a continuous vacuum rotary drum filter.

13.1.1 Filtrate Flow Through Filter Cake

In filter aid filtration, filtrate flow through the pores in the cake is dependent on the pressure differential across the cake and the resistance to flow. The total resistance increases with increasing cake thickness, thus filtrate flow decreases with time of filtration. The resistance to filtrate flow across the filter cake is expressed as the specific cake resistance.

Figure 13.3 shows a section of a filter showing the filter medium, precoat, and filter aid. The total pressure drop across the filter is the sum of the pressure drop across the filter medium (the filter cloth and precoat), ΔP_m , and that across the cake, ΔP_c .

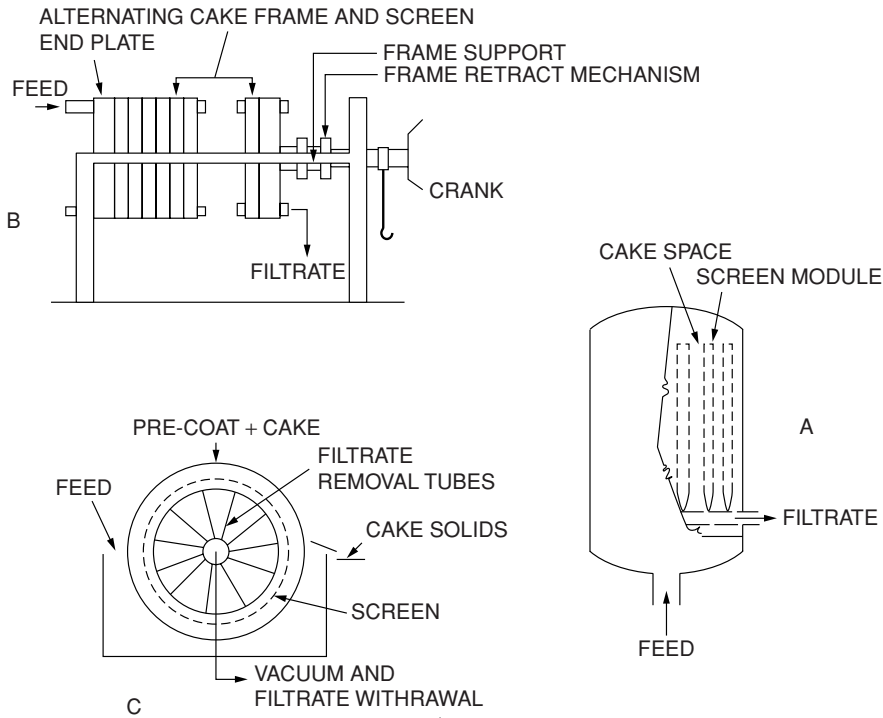


Figure 13.2 Diagram of common filters for filter aid filtration. (A) vertical leaf filter; (B) plate and frame filter; (C) rotary vacuum drum filter.

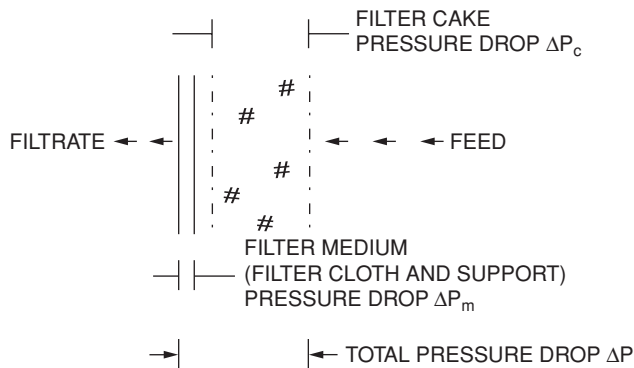


Figure 13.3 Diagram of a filter section showing filter cloth, precoat, and filter cake.

Let v = velocity of filtrate flow, μ = filtrate viscosity, A = filter area, and m = mass of filter cake. The medium resistance, R_m , is

$$R_m = \frac{\Delta P_m}{\mu v} \quad (13.1)$$

The specific cake resistance, α , is

$$\alpha = \frac{\Delta P_c}{\mu v(m/A)} \quad (13.2)$$

The units of R_m and α are m^{-1} and m/kg , respectively, in SI.

Let: ΔP = pressure differential across the filter

$$\Delta P = \Delta P_m + \Delta P_c \quad (13.3)$$

Substituting Equations (13.1) and (13.2) in Equation (13.3):

$$\Delta P = \alpha \mu v \frac{m}{A} + R_m \mu v \quad (13.4)$$

Let: V = volume of filtrate and c = concentration of cake solids in the suspension to be filtered. $m = Vc$. The filtrate velocity, $v = (1/A) dV/dt$.

Substituting for m and v in Equation (13.4):

$$\Delta P = \frac{\mu(dV/dt)}{A} \left[\frac{\alpha Vc}{A} + R_m \right] \quad (13.5)$$

$$\frac{dt}{dV} = \frac{\mu}{A \cdot \Delta P} \left[\frac{\alpha Vc}{A} + R_m \right] \quad (13.6)$$

Equation (13.6) is the Sperry equation, the most widely used model for filtrate flow through filter cakes. Equation (13.6) can be used to determine the specific cake resistance from filtration data. Filtration time, t , is plotted against filtrate volume, V , tangents to the curve are drawn at several values of V , and the slopes of the tangents, dt/dV , are determined. A plot of dt/dV versus V will have a slope equal to $\alpha c \Phi(A^2 \cdot \Delta P)$ and an intercept on the ordinate at $V = 0$ equal to $R_m \Phi(A \cdot \Delta P)$. An easier method for determining α and R_m will be shown in next section.

13.1.2 Constant Pressure Filtration

When a centrifugal pump is used as the filter feed pump, the pressure differential across the filter, ΔP , is constant, and Equation (13.6) can be integrated to give:

$$t = \frac{\mu}{\Delta P} \left[\frac{\alpha c}{2} \frac{V^2}{A^2} + R_m \frac{V}{A} \right] \quad (13.7)$$

Dividing Equation (13.7) through by V :

$$\frac{t}{V} = \frac{\mu \alpha c}{2A^2 \Delta P} V + \frac{\mu R_m}{A \Delta P} \quad (13.8)$$

Equation (13.8) shows that a plot of t/V against V will be linear, and the values of α and R_m can be determined from the slope and intercept. A common problem with the use of either Equation (13.6) or Equation (13.8) is that negative values for R_m may be obtained. This may occur when R_m is much smaller than α ; if finely suspended material is present that rapidly reduces medium porosity even with very small actual amount of cake solids deposited; or when α increases with time of filtration such that

the least squares method of curve fitting weighs heavily the data during the later stages of filtration relative to those at the early stages. To avoid having negative values for R_m , Equation (13.7) may be used in the analysis. If filtration is carried out using only filtrate containing no suspended solids, $c = 0$ and equation 7 becomes:

$$t = \frac{\mu R_m}{\Delta P A} V \quad (13.9)$$

Because $R_m = \Delta P_m / (\Phi \cdot v)$; and since during filtration with only the filter cloth and precoat, the pressure differential is ΔP_m , and because $A \cdot v =$ the filtrate volumetric rate of flow, q , the coefficient of V in Equation (13.9) is $1/q$. Thus, Equation (13.7) can be expressed as:

$$t = \frac{\mu \alpha c}{2 \Delta P A^2} V^2 + \left(\frac{1}{q} \right) V \quad (13.10)$$

q is evaluated separately as the volumetric rate of filtrate flow on the precoat filter at the pressure differential used in filtration with body feed. Because ΔP across the precoat filter is primarily due to the resistance of the deposited filter aid, q is primarily a function of the type of filter aid, the pressure applied, and the thickness of the cake. For the same filter aid and filtrate, q is proportional to the thickness and the applied pressure, therefore the dependence can be quickly established. If q is known, α can be easily determined from the slope determined by a regression of the function $(t - V/q)$ against V^2 or from the intercept of a log-log plot of $(t - V/q)$ against V .

The use of filtration model equations permits determination of the filtration constants R_m and α on a small filter which can then be used to scale up to larger filtrations. An example of a laboratory filtration module is shown in Fig. 13.4. This is a batch filter with a tank volume of 7.5 L and a filter

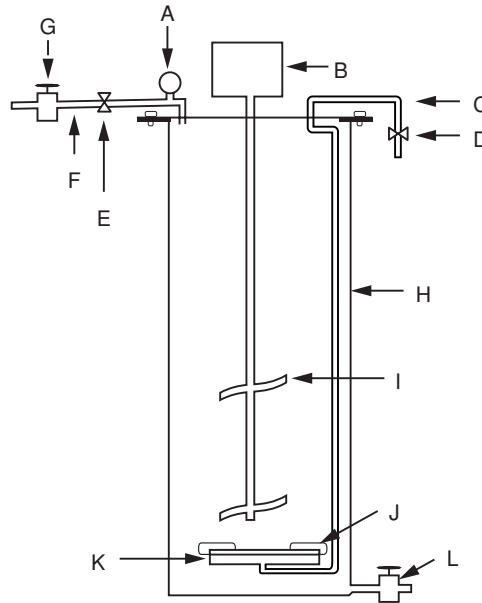


Figure 13.4 Diagram of a laboratory test filtration cell.

Table 13.1 Data for Filtration Clarification of Apple Juice.

Time $t(s)$	Filtrate Volume $V(m^3) \times 10^5$	$t/V \times 10^{-6}$
60	3.40	1.7647
120	5.80	2.0689
180	7.80	2.3077
240	9.60	2.5000
300	11.4	2.6316
360	13.1	2.7586
420	14.7	2.8669
480	16.1	2.9721
540	17.6	3.0769
600	19.0	3.1496
660	20.6	3.2117
720	22.0	3.2727
780	23.3	3.3476

area of 20 cm^2 . An opening at the bottom allows draining of the precoat suspension at the beginning of a filtration cycle, and charging of the tank after precoat. To precoat, a suspension of filter aid is made at such a concentration that filtration of 1000 mL will give the precoat level of 1.0 kg/m^2 . For example, 2.0 g dry filter aid in 1000 mL of water will be equivalent to a precoat of 1.0 kg/m^2 on a filter area of 20 cm^2 if 1000 mL of filtrate is allowed to pass through the filter from this suspension. Depending upon the fineness of the filter aid used, filter paper, or cloth may be used as the filter medium.

Example 13.1. Data in Table 13.1 were collected in filtration clarification of apple juice. The apple juice was squeezed from macerated apples, treated with pectinase, and after settling and siphoning of the clarified layer, the cloudy juice that remained in the tank was filter clarified using perlite filter aid. The cloudy juice contained 1.19 g solids/100 mL. Perlite filter aid was used which had a pure water permeability of $0.40 \text{ mL} \cdot \text{s}^{-1}$ for 1 cm^2 filter area, 1 atm pressure drop and 1 cm thick cake. Whatman no. 541 filter paper was used as the filter medium. The precoat was 0.1 g/cm^2 (1 kg/m^2). The filter shown in Fig. 13.4, which had a filtration area of 20 cm^2 , was used. Flow of clear apple juice through the precoat filter was 0.6 mL/s at a pressure differential of $25 \text{ lb}_f/\text{in.}^2$ (172.369 kPa). The filtrate had a viscosity of 1.6 cP .

Calculate α and R_m . Calculate the average filtration rate in $\text{m}^3/(\text{min} \cdot \text{m}^2 \text{ filter area})$ if the filtration time per cycle is 30 min and the pressure differential across the filter is $30 \text{ lb}_f/\text{in.}^2$ (206.84 kPa). Assume the same solids and body feed concentration.

The cumulative filtrate volume with filtration time at a filter aid concentration of 2.5 g/100 mL of suspension, is shown in Table 13.1.

Solution:

Using Equation (13.8), a regression of (t/V) against V was done using the transformed data in Table 13.1.

The regression equation was:

$$(t/V) = 7.61 \times 10^9 V + 1,684,000$$

The coefficient of V is $\alpha \cdot \mu \cdot c / (2\Delta P A^2)$. c = concentration of filter cake solids in the feed, which is the sum of the original suspended solids, 1.19 g/100 mL or 11.9 g/L, and the body feed filter aid concentration which is 2.5 g/100 mL or 25 g/L.

$$\alpha = \frac{7.61 \times 10^9 (2)(20 \times 10^{-4})^2 (172,369)}{1.6(0.001)925 + 11.9} = 1.78 \times 10^{11} \text{ m/kg}$$

The intercept is $R_m \mu / (A \Delta P)$

$$R_m = \frac{1.684 \times 10^6 (20 \times 10^{-4}) (172,369)}{0.001(1.6)} = 3.63 \times 10^{11} \text{ m}^{-1}$$

Similar values for α and R_m were obtained using Equation (13.10) by performing a regression on $(t - V/q)$ against V^2 . q is $0.6 \times 10^{-6} \text{ m}^3/\text{s}$. A slightly better fit was obtained using Equation (13.10) with $R^2 = 0.994$ compared with $R^2 = 0.964$ using Equation (13.8). The regression equation using Equation (13.10) was:

$$(t - V/q) = 7.29 \times 10^9 V^2$$

Values for R_m and α were 3.59×10^{11} and 1.7×10^{11} , respectively, in SI units. These values would be more accurate than those obtained using equation 8 because of the better R^2 value for the regression. However, the values are very close and would be considered the same for most practical purposes.

The average filtrate flow is calculated using Equation (13.7). $t = 30 \text{ min} = 1800 \text{ s}$

$$1800 = \frac{1.6(0.001)}{206,840} \left(\frac{1.78 \times 10^{11} \times (36.9)}{2} \left[\frac{V}{A} \right]^2 + 3.63 \times 10^{11} \left[\frac{V}{A} \right] \right)$$

$$32.841 \times 10^{11} (V/A)^2 + 3.63 \times 10^{11} (V/A) = 2.32698375 \times 10^{11}$$

Dividing through by 32.841×10^{11} and solving for the positive root of the quadratic equation

$$(V/A)^2 + 0.1105(V/A) - 0.070856 = 0$$

$$\frac{V}{A} = \frac{-0.1105 \pm ([0.1105]^2 + 4(1)(0.070856))^{0.5}}{2} = 0.217 \text{ m}^3/\text{m}^2 \text{ filter area}$$

This is the volume of filtrate which passed through a unit area of the filter for a filtration cycle of 30 min. The average rate of filtration is

$$(V/A)_{\text{avg}}/t = 0.217/30 = 0.00722 \text{ m}^3/(\text{min} \cdot \text{m}^2 \text{ filter area})$$

The average filtration rate can be used to size a filter for a desired production rate if the same filtration cycle time is used.

Two approaches were used to evaluate R_m and α in example 13.1. In both approaches, the traditional graphical method for determining filtration rate by drawing tangents to the filtration curve was eliminated. In this example, the resistance of the filter medium was the same magnitude as the specific cake resistance, therefore, the Sperry equation worked well in determining R_m . There are instances, particularly when $R_m \ll \alpha$, when a negative intercept will be obtained using Equation (13.8). Under these conditions, R_m is best determined by filtration of solids-free filtrate to obtain q , and using

Equation (13.10) to determine α . In the above example, use of the values of α and R_m calculated using Equation (13.10), will give a filtrate volume per 30 minutes cycle of $0.221 \text{ m}^3/\text{m}^2$ of filter area, or an average filtration rate of $0.00737 \text{ m}^3/(\text{min} \cdot \text{m}^2 \text{ filter area})$.

13.1.3 Filtration Rate Model Equations for Prolonged Filtration When Filter Cakes Exhibit Time-Dependent Specific Resistance

Equation (13.6) and variations on it such as Equation (13.7) are used assuming that specific cake resistance is constant. These equations usually provide good fit with experimental filtration data for short filtration times as was shown in the previous example. However, when filtration time is extended, Equation (13.8) usually overestimates the filtrate flow. Some filter cakes undergo compaction or fine solids may migrate within the pores blocking flow and increase cake resistance as filtration proceeds.

13.1.4 Exponential Dependence of Rate on Filtrate Volume

The Sperry equation has been modified to account for changing resistance with increasing filtration time. de la Garza and Bouton (Am. J. Enol. Vitic. 35:189, 1984) assumed α to be constant and modified the Sperry equation such that the filtration rate is a power function of filtrate volume.

$$\frac{dt}{dV} = \frac{\mu}{\Delta P A} \left(\alpha c \left[\frac{V}{A} \right]^n + R_m \right) \quad (13.11)$$

Integration of Equation (13.11) gives:

$$t = \frac{\mu}{\Delta P A} \left(\frac{\alpha c}{n+1} \left[\frac{V}{A} \right]^{n+1} + R_m V \right) \quad (13.12)$$

Bayindirly et al. (J. Food Sci. 54:1003, 1989) tested Equation (13.12) on apple juice and found that a common n in Equation (13.11) could not be found to describe all data at different body feed concentrations. Consequently, an alternative equation was proposed which combines the specific cake resistance and solids concentration into a parameter k .

$$\frac{dt}{dV} = \frac{\mu}{A \Delta P} R_m [e]^{kV/A} \quad (13.13)$$

Integration of Equation (13.13) gives:

$$t = \frac{\mu}{k \Delta P} R_m [e]^{kV/A} \quad (13.14)$$

Taking the natural logarithm of Equation (13.14):

$$\ln(t) = \ln \left[\frac{\mu R_m}{k \Delta P} \right] + \frac{k}{A} V \quad (13.15)$$

A semi-log plot of t against (V/A) will be linear with slope k . R_m is evaluated from the intercept.

Example 13.2. Data in Table 13.2 was obtained from Bayindirly et al. on filtration of apple juice through a filter with a 30.2 cm^2 area using diatomaceous earth filter aid with an average particle size

Table 13.2 Filtration Data for Apple Juice.

Time (s)	$\ln(t)$	Filtrate Volume		
		$V(\text{m}^3) \times 10^5$	$t/V \times 10^{-6}$	$t - (V/q)$
84.3	4.353	9.74	8.659	14.78
112.5	4.723	12.3	9.141	24.59
140.6	4.946	14.4	9.793	38.06
196.9	5.283	17.4	11.291	72.33
281.2	5.639	20.0	14.062	138.39
421.9	6.045	22.6	18.697	260.70
759.4	6.632	27.2	27.939	565.24
1068.8	6.974	29.7	35.932	856.29
1575	7.362	32.3	48.750	1344.2
2250	7.719	24.9	64.522	2000.9
3825	8.249	39.5	96.867	3542.9

of 20 μm . The juice was said to have a viscosity just slightly greater than that of water (assume $\mu = 1.0 \text{ cP}$) and suspended solids in the juice was 0.3% (3.0 kg/m^3). Precoating was 0.25 g/cm^2 (2.5 kg/m^2) and body feed was 0.005 g/mL (5.0 kg/m^3). Pressure differential was 0.65 atm. Calculate the filtration parameters, k and R_m and the average filtration rate in $\text{m}^3/(\text{min} \cdot \text{m}^2 \text{ of filter area})$, if a filtration cycle of 60 min is used in the filtration process.

Solution:

Table 13.2 also shows the transformed data on which a linear regression was performed. Linear regression of (t/V) against V to fit Equation (13.8) results in the following correlation equation:

$$t/V = 2.64 \times 10^{10}V - 3,107,386$$

The problem of a negative value for the term involving the medium resistance, R_m is apparent in the analysis of this data. The correlation coefficient was 0.835 which may indicate reasonable fit, however, when filtration time against filtrate volume is plotted the lack of fit is obvious. Thus, the Sperry equation could not be used on the data for this filtration.

A linear regression of $\ln(t)$ against V according to Equation (13.15) results in the following regression equation:

$$\ln(t) = 13155.92V + 3.70293$$

The correlation coefficient was 0.998 indicating very good fit. A plot of filtration time against filtrate volume also shows very good agreement between values calculated using the correlation equation and the experimental data. The exponential dependence of filtration rate with filtrate volume appropriately described the filtration data.

The value of k is determined from the coefficient of V in the regression equation.

$$k/A = 13155.92; \quad k = 13155.92(30.2 \times 10^{-4})$$

$$k = 39.73 \text{ m}^{-1}$$

The constant, 3.70293 in the regression equation is the value of $\ln(\mu R_m/k \cdot \Delta P)$

$$R_m = \frac{e^{3.70293} (39.73)(0.65)(101,300)}{0.001(1)} = 5.652 \times 10^{10} \text{ m}^{-1}$$

The correlation equation will also be used to calculate the filtrate volume after a filtration time of 60 minutes.

$$V = \frac{\ln(3600) - 3.70293}{13155.92} = 0.000348 \text{ m}^3$$

Average filtration rate = $(V/A)_{\text{avg}}/t$

$$\frac{(V/A)_{\text{avg}}}{t} = \frac{0.000341}{(30.2 \times 10^{-4})(60)} = 0.001882 \text{ m}^3/(\text{min} \cdot \text{m}^2 \text{ filter area})$$

13.1.5 Model Equation Based on Time-Dependent Specific Cake Resistance

Chang and Toledo (J. Food Proc. Pres. 12:253, 1989) modified Equation (13.10), derived from the Sperry equation, by assuming a linear dependence of the specific cake resistance with time. The model fitted experimental data on body feed filtration of poultry chiller water overflow for recycling, using perlite filter aid.

$$t = (k_0 + \beta t)V^2 + (1/q)V \quad (13.16)$$

The ratio $(t - V/q)/V^2$ is $(k_0 + \beta t)$ at each filtration time t . The slope of the regression equation of $(t - V/q)/V^2$ against filtration time will have a slope of β and an intercept of k_0 . The filtrate volume at time t will be the positive root of Equation (13.16).

$$V = \frac{-(1/q) + [(1/q)^2 + 4(k_0 + \beta t)t]^{0.5}}{2(k_0 + \beta t)} \quad (13.17)$$

Filtration data may be analyzed using this procedure by using the raw volume vs. time data, and the filter area is not considered until the final analysis (i.e., calculated value of filtrate volume or filtration rate is converted to a per unit area basis). Another approach is to use filtrate volume per unit area of filter in the calculations, in which case the calculated value of filtrate volume will already be on a per unit area basis. The former approach is used in the following example to avoid having to manipulate very small numbers.

The units of k_0 and β in Equation (13.16) are $\text{s} \cdot \text{m}^{-6}$ and m^{-6} , respectively, because values of V used in the analysis have not been converted to Volume/filter area.

Example 13.3. Table 13.3 shows data on filtration of poultry chiller water overflow using perlite filter aid which has a rated pure water permeability of $0.4 \text{ mL}/(\text{s} \cdot \text{m}^2)$ for a 1 cm cake and a 1 atm pressure differential. The filter has an area of 20 cm^2 , water at 2°C was the filtrate. The precoat was $1.0 \text{ kg}/\text{m}^2$ of filter area. Whatman no. 541 filter paper was used as the filter medium. Body feed was $5 \text{ kg}/\text{m}^3$ and suspended solids was $5 \text{ kg}/\text{m}^3$. Pressure across the filter was 172 kPa. Filtrate flow across the precoated filter was $25.5 \text{ mL}/\text{s}$ at 172 kPa pressure differential. Calculate the parameters for the time dependence of specific cake resistance and determine the fit of Equation (13.16) with experimental data. Calculate the average filtration rate if the cycle time is 20 min.

Table 13.3 Data on Filtration of Poultry Chiller Water.

Time (s)	Volume of Filtrate $V(\text{m}^3)$	$t - V/q$	$R = (t - V/q)/V^2$ $\times 10^8$
60	0.000483	41.059	1.760
180	0.000823	147.7	2.181
300	0.001031	259.6	2.442
420	0.001173	374.0	2.718
540	0.001292	489.3	2.931
660	0.001385	605.7	3.156
780	0.001466	722.5	3.362
900	0.001538	839.7	3.550
1020	0.001601	957.1	3.734
1140	0.001658	1075.0	3.910
1200	0.001660	1134.9	4.118

$q = 25.5 \times 10^{-6} \text{ m}^3/\text{s}$

Solution:

Table 13.3 also shows the values of $(t - V/q)/V^2$ on which a regression analysis was done against time to yield the following regression equation ($R^2 = 0.9883$)

$$k_0 + \beta t = 191,347t + 1.83 \times 10^8 \quad (13.17a)$$

Table 13.4 shows the calculation of filtrate volume against filtration time using the expression for $k_0 + \beta t$ in Equation (13.17a) and Equation (13.17). A graph of calculated filtrate volume against filtration time shows good agreement between the model and experimental value.

For a filtration time of 20 minutes, the calculated value of V in Table 13.4 is 0.001659 m^3 . The average filtration rate is

$$(V/A)_{\text{avg}}/t = 0.001659/[(20)(20 \times 10^{-4})]$$

$$(V/A)_{\text{avg}}/t = 0.0415 \text{ m}^3/(\text{s} \cdot \text{m}^2 \text{ filter area})$$

at 172 kPa pressure differential across the filter.

13.1.6 Optimization of Filtration Cycles

Filtration cycles are generally based on obtaining the fastest average filtrate flow. As filtrate flow drops with increasing cake thickness, a very long filtration time will result in the lowered average filtration rate. However, labor involved in disassembling the filter, removal of the cake, and pre-coating will be a major expense. Because pre-coating is needed before actual filtration, shortened filtration cycles will necessitate increased consumption of filter aid. Thus, optimum cycles based on maximum filtrate flow, may not always be the ideal cycle time from the standpoint of economics. Filtrations with short cycle times for maximum filtrate flow per unit filter area may have to be done

Table 13.4 Calculation of Filtrate Volume from Cake Resistance Data.

<i>Time (s)</i>	$k_0 + \beta t \times 10^{-8}$	$1/q$	$C \times 10^{-10}$	<i>Filtrate Volume (V) Calculated from Equation 17 (mL)</i>
60	1.94	39215	4.82	464
180	2.17	39215	15.8	824
300	2.40	39215	29.0	1038
420	2.63	39215	44.4	1191
540	2.86	39215	62.0	1307
660	3.09	39215	81.8	1399
780	3.32	39215	104	1474
900	3.55	39215	128	1537
1020	3.78	39215	154	1591
1140	4.01	39215	183	1637
1200	4.13	39215	198	1659

$q = 2.55 \times 10^{-5}$; From equation 17: $C = (1/q)^2 + 4(k_0 + \beta t)$;
 $V = [-(\text{column 2}) + (\text{column 3})^{0.5}]/[2 \text{ column 1}]$.

using a continuous rotary vacuum filter to prevent excessive filter aid use. The optimum cycle time for maximizing filtrate flow per cycle is derived as follows.

For filtrations that fit the Sperry equation (Eq. 13.7):

A cycle is the sum of filtration time, t and the time to disassemble, assemble and precoat the filter t_{DAP} .

$$\frac{V}{\text{Cycle}} = \frac{V}{t + t_{\text{DAP}}}$$

Let $k_1 = \pi \alpha c / 2 \Delta P$; and $k_2 = R_m \pi / \Delta P$. Equation 7 becomes:

$$t = k_1(V/A)^2 + k_2(V/A)$$

To obtain the optimum cycle time, the filtrate volume per cycle is maximized by taking the derivative and equating to zero as follows:

$$\frac{d}{dV} \left[\frac{V}{t + t_{\text{DAP}}} \right] = \frac{d}{dV} \left[\frac{V}{k_1(V/A)^2 + k_2(V/A) + t_{\text{DAP}}} \right]$$

The derivative is equated to zero to obtain V/A for the maximum V/cycle .

$$0 = \frac{[k_1(V/A)^2 + k_2(V/A) + t_{\text{DAP}}] - V[2k_1(V/A) + k_2/A]}{[k_1(V/A)^2 + k_2(V/A) + t_{\text{DAP}}]^2}$$

$$t_{\text{DAP}} - k_1(V/A)^2 = 0$$

$$\left(\frac{V}{A} \right)_{\text{max}} = \left[\frac{t_{\text{DAP}}}{k_1} \right]^{0.5}$$

The optimum cycle time, t_{opt} is

$$\begin{aligned}
 t_{\text{opt}} &= k_1 \left[\frac{t_{\text{DAP}}}{k_1} \right] + k_2 \left[\frac{t_{\text{DAP}}}{k_1} \right]^{0.5} \\
 t_{\text{opt}} &= t_{\text{DAP}} + k_2 \left[\frac{t_{\text{DAP}}}{k_1} \right]^{0.5} \\
 t_{\text{opt}} &= t_{\text{DAP}} + R_m \left[\frac{2\mu t_{\text{DAP}}}{\alpha c \Delta P} \right]^{0.5}
 \end{aligned} \tag{13.18}$$

When filtration data fits Equation (13.14), the (V/A) for maximum filtrate flow derived using the above procedure, is the root of Equation (13.19):

$$\mu R_m (e)^{k \left[\frac{V}{A} \right]} \left(\frac{k}{A^2} - \frac{V}{A} \right) - t_{\text{DAP}} = 0 \tag{13.19}$$

When filtration data fits Equation (13.16), t as a function of k_0 , V , and q only, is solved as follows:

$$t = \frac{k_0 V^2 + q^{-1} V}{1 - \beta V^2}$$

The optimum V for one filtration cycle is the root of Equation (13.20).

$$V^4(\beta k_0) + V^3(2\beta q^{-1}) + V^2(k_0 + 2\beta t_{\text{DAP}}) - t_{\text{DAP}} = 0 \tag{13.20}$$

Example 13.4. Calculate the optimum filtration cycle in example 13.3 for poultry chiller water overflow filtration, to maximize filtrate flow, assuming 10 min. for disassembly, assembly and pre-coating. Use the values, $k_0 = 1.83 \times 10^8 \text{ s/m}^6$; $\beta = 191,347 \text{ l/m}^6$; $q = 25.5 \times 10^{-6} \text{ m}^3/\text{s}$ calculated in Example 13.3.

Solution:

The values of k_0 , β , q and $t_{\text{DAP}} = 600 \text{ s}$ are substituted in Equation (13.20), which is then solved for V . A Visual BASIC program will be used to solve for the optimum filtrate volume, V , and the filtration time. The first 5 lines in the program assigns the known values of β , k_0 , q , and t_{DAP} , followed by Equation (13.20), and then the equation solves for t required for filtrate volume V to flow through the filter. Figure 13.5 shows the program and the output.

The value of $F = -1.046$ when $V = 0.001122$, and $F = 0.143$ when $V = 0.001123$. Thus, the optimum V for a cycle will be 0.001123 m^3 or 1123 mL . The optimum cycle time is 370 s .

The filtration behavior shown in this example results in very short cycle times because of very rapid loss of filter cake porosity. Thus, use of a batch filter in carrying out this filtration will result in excessive filter aid use. Use of a continuous rotary vacuum filter is indicated for this application.

13.1.7 Pressure-Driven Membrane Separation Processes

A form of filtration that employs permselective membranes as the filter medium is employed to separate solute, macromolecules, and small suspended particles in liquids. A thin membrane with small pore size, which possesses selectivity for passing solute or solvent, is used. The solvent and small molecules pass through the membrane and other solutes, macromolecules or suspended solids are

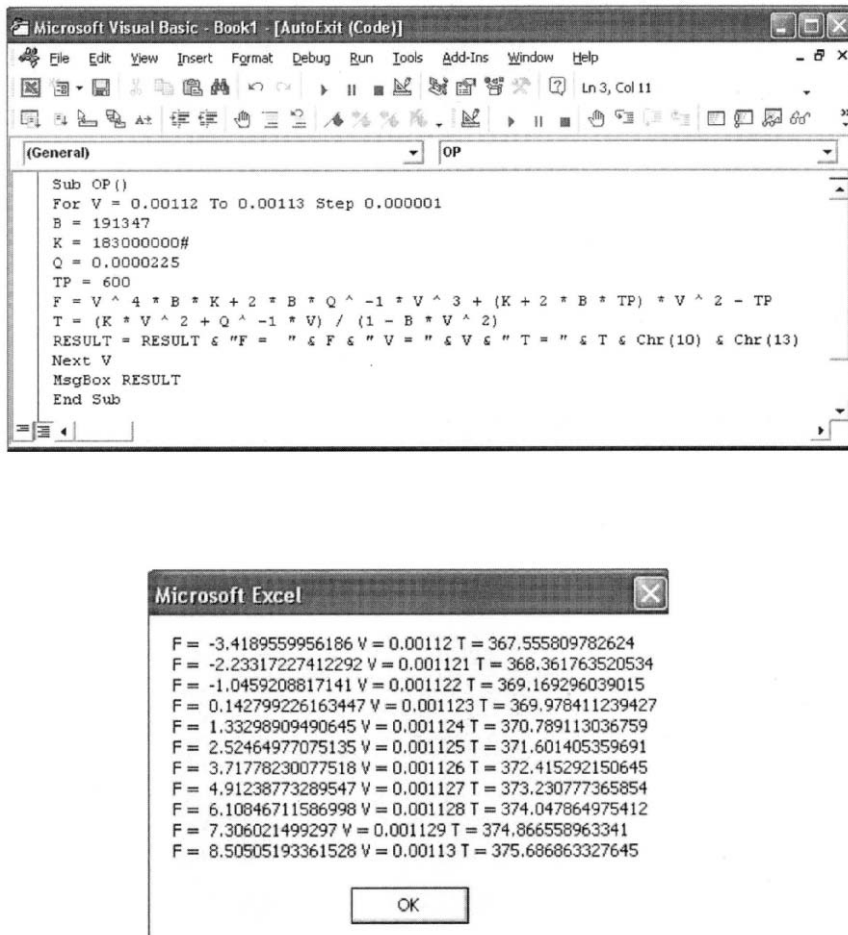


Figure 13.5 Visual BASIC program for calculating optimum filtration cycle times.

retained either by repulsive forces acting on the membrane surface or by a sieving effect. Figure 13.6 shows a typical membrane filtration system. Cross-flow filtration is the most efficient configuration, as discussed later, and retentate recycling is needed to obtain both high cross-membrane fluid velocities and the desired final solids concentration in the product. The fluid crossing the membrane is the “permeate” and the fluid retained on the feed side of the membrane is the “retentate.” The fluid entering the membrane is the “feed.”

Pressure driven membrane separation processes include:

Microfiltration (MF): particle size retained on the membrane is in the range of 0.02 to 10 μm .

Sterilizing filtration is a MF process.

Ultrafiltration (UF): particle size retained on the membrane is in the range of 0.001 to 0.02 μm .

Concentration of cheese whey and removal of lactose is a UF process.

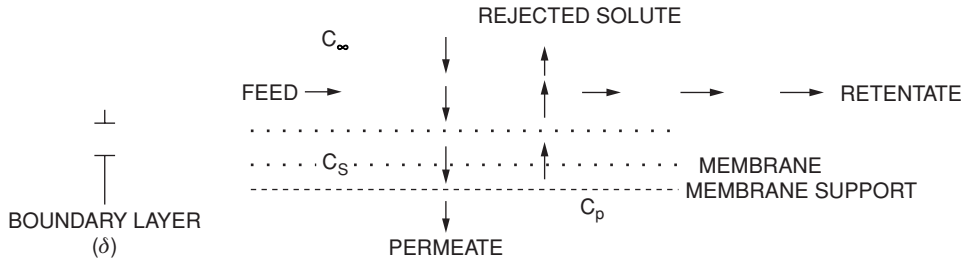


Figure 13.6 Cross-section of a membrane in ultrafiltration.

Reverse osmosis (RO): solute molecules with molecular size less than $0.001 \text{ } \mu\text{m}$ (molecular weight <1000 daltons) are retained on the membrane surface. In RO, solutes increase the osmotic pressure, therefore the transmembrane pressure is reduced by the osmotic pressure as the driving force for solvent flux across the membrane. Concentration of apple juice and desalination of brackish water are examples of RO processes.

Membranes are either isotropic or anisotropic. An isotropic membrane has uniform pores all the way across the membrane thickness, while an anisotropic membrane consists of a thin layer of permselective material on the surface and a porous backing. MF membranes may be isotropic or anisotropic, while permselective high flux membranes used in UF and RO are primarily anisotropic. Membranes are formed by casting sheets using a polymer solution in a volatile solvent followed by evaporation of the solvent. Removal of the solvent leaves a porous structure in the membrane. Larger pore size membranes are produced by subjecting a nonporous polymeric membrane to high-energy radiation. The polymer is changed at specific points of entry of the radiation into the membrane. A secondary treatment to dissolve the altered polymer produces pores within the membrane. Dynamic casting may also be employed. A porous support is coated with the membrane material by pumping a solution containing the membrane material across its surface. As the solvent filters across the porous support, the membrane material is slowly deposited. Eventually, a layer with the desired permselectivity is produced.

Two major factors are important in the design and operation of pressure driven membrane separation processes. These are transmembrane flux and solute rejection properties of the membrane. In general, transmembrane flux and rejection properties are dependent on properties of solute and suspended solids and membrane characteristics of (a) mean pore size, (b) range of pore size distribution, (c) tortuous path for fluid or particle flow across the membrane thickness or “tortuosity,” (d) membrane thickness, and (e) configuration of pores. Operating conditions also affect flux and rejection of solutes, and this will be discussed in the succeeding sections.

13.1.8 Membrane System Configurations

The effectiveness of membrane systems may be measured by effectiveness in separating the component of interest at a high production rate. Regardless of whether the valuable component is in the retentate or in the permeate, transmembrane flux must be maximized. Because flux is a function of pressure and membrane area, and is constrained by fouling, the different membrane system

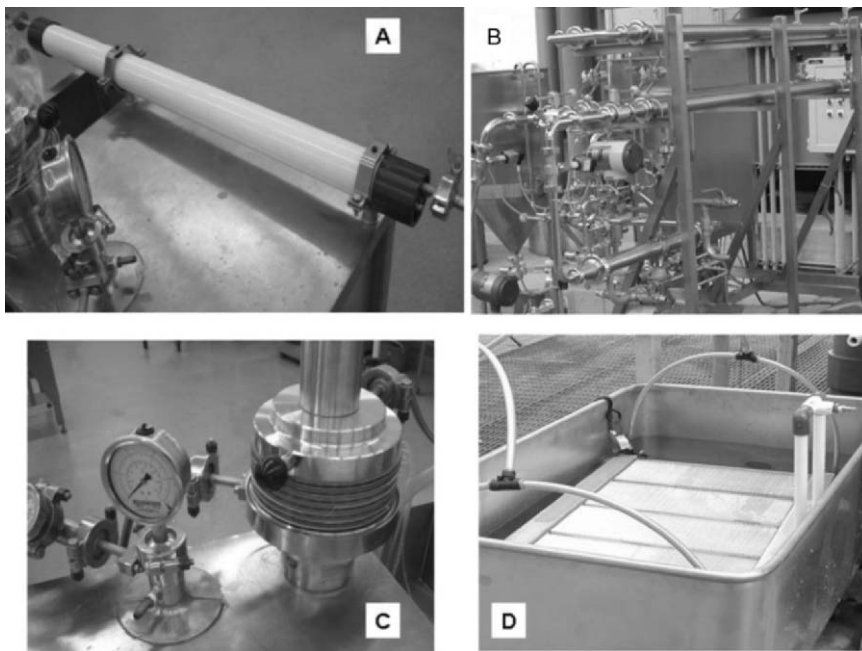


Figure 13.7 Membrane system configuration.

configurations available are designed to maximize membrane area within a small footprint, operate at high pressure, minimize fouling, and facilitate cleaning. Figure 13.7 shows four different membrane system configurations. The spiral wound membrane (Fig. 13.7A) is the most commonly used configuration. The membrane module is tubular with channels between the spiral wound sheet for feed to flow across the membrane from one end of the tube to the opposite end. A spacer sheet between the membrane layer on the permeate side permits permeate to travel around the spiral until it enters the permeate tube at the center of the spiral. The tubular spiral wound module is placed inside a tubular pressure vessel. This configuration permits the most effective packing of a large membrane area in a small space. The disadvantage is the tendency to trap solid particles in the spaces within the spiral thus making it difficult to clean. Feed to a spiral wound membrane system must be pre-filtered to remove particles that could get trapped in the module. The use of spiral wound membranes has made it possible to economically produce potable water from sea water in large desalination plants.

Tubular membranes (Fig. 13.7B) made of ceramic material or inorganic solids deposited on a porous stainless steel support require a large footprint for a given membrane surface area. They have the advantage of being able to operate at high pressure and temperature, resist cleaning compounds, and permit back-flushing to dislodge foulant that penetrated the pores. These membranes have high first cost but membrane life is considerably longer than the polymeric membranes.

Plate and frame membrane units (Fig. 13.7C) permit stacking of several membrane sheets to form a compact unit with large membrane surface area. Plates with the membrane material deposited on each surface are available and when these plates are used, the unit is easily disassembled for cleaning. The

manufacturer also supplies membrane support frames which permits a user to use flat sheet membranes on the unit.

A modular submerged module membrane unit is shown in Fig. 13.7D. The module consists of stacks of multiple envelope-like membrane elements arranged in a very compact configuration. Each element consists of two sheets of membrane material with a spacer between them. The edges of the membrane sheets are welded together to prevent feed from entering the element. An opening in the center of the element permits stacking them with gaskets in-between through a permeate removal tube. Because of the large membrane surface area, these units require very low transmembrane pressure to obtain the desired flux. Air scouring of the membrane surface prevents fouling.

Other configurations such as hollow fiber bundles, vibrating membrane units, and cartridge modules are also available and are used in industry.

13.1.9 Transmembrane Flux in Pressure-Driven Membrane Separation Processes (Polarization Concentration and Fouling)

Qualitatively, similarities exists in ordinary filtration and membrane separation processes. The net transmembrane pressure, which drives solvent flow across the membrane, is the sum of the pressure drop across the filter medium, ΔP_m , and the pressure drop across the combined deposited solids on the surface and the boundary layer of concentrated suspension flowing across the membrane surface, ΔP_δ . The development of the equation for transmembrane flux will be similar to that for filtration rate in filter aid filtrations. The pure water permeability of the membrane usually given by the membrane manufacturer, is q in Equation (13.10).

Transmembrane flux when a compressible deposit is on the membrane may be expressed by modifying the Sperry equation (Eq. 13.6) by letting $\alpha = \alpha_0 \Delta P^n$ as follows:

$$\frac{dV}{dt} = \frac{Aq\Delta P}{\mu\alpha_0\Delta P^n cq(V/A) + A\Delta P} \quad (13.21)$$

n is a compressibility factor that is 0 for a completely incompressible and 1 for a completely compressible solid deposit. q is the pure water permeability at the transmembrane pressure used in the filtration, ΔP .

If the second term in the denominator is much smaller than the first term, i.e., the resistance of the deposit and the fluid boundary layer at the membrane surface controls the flux, Equation (13.21) becomes:

$$\frac{dV}{dt} = \frac{A^2 \Delta P^{1-n}}{\mu\alpha_0 c V} \quad (13.22)$$

Equation (13.22) shows that if n is 1 (i.e., the solid deposit is completely compressible), the transmembrane flux is independent of the transmembrane pressure. This phenomenon has been observed in UF and RO operations. For example, in UF of cheese whey, transmembrane flux is proportional to pressure at transmembrane pressure between 30 and 70 lb_f/in.² gauge (207 to 483 kPa) and is independent of pressure at higher pressures. The phenomenon of decreasing flux rates with increased permeate throughput V , shown in Equation (13.22), has also been observed. Solids deposition on the membrane surface is referred to as “fouling.”

Even in the absence of suspended solids, transmembrane flux with solutions will be different from the pure water permeability. This decrease in flux is referred to as “polarization concentration.” In simplistic terms, Equation (13.22) qualitatively expresses the phenomenon of polarization concentration

in membrane filtrations. As solvent permeates through the membrane, the solids concentration, c , increases in the vicinity of the membrane. The transmembrane flux is inversely proportional to the solids concentration in Equation (13.22).

The concentration on the membrane surface increases with increasing transmembrane flux, therefore, the phenomenon of flux decrease due to polarization concentration will be more apparent at high transmembrane flux. Flux decrease due to polarization concentration is minimized by increasing flow across the membrane surface by cross-flow filtration. In the absence of suspended solids which form fouling deposits, flux will be a steady state. In the presence of suspended solids which form compressible deposits, flux will continually decrease with increasing throughput of permeate, V .

Flux decrease due to polarization concentration is a function of the operating conditions, and if flow rate on the membrane surface, solids concentration in the feed, and transmembrane pressure are kept constant, flux should remain constant. Flux decline under constant operating conditions can be attributed to membrane fouling.

Porter (1979) presented theoretical equations for evaluation of polarization concentration in ultra-filtration and reverse osmosis. The theoretical basis for the equations is the mass balance for solute or solids transport occurring at the fluid boundary layer at the membrane surface.

In cross-flow filtrations, fluid flows over the membrane at a fast rate. A laminar boundary layer of thickness δ exists at the membrane surface. If C is the solids concentration in the boundary layer, and C_4 is the concentration in the liquid bulk, a mass balance of solids entering the boundary layer with the solvent and those leaving the boundary layer by diffusion will be

$$\left(\frac{\partial V}{\partial t}\right)C = -D\left(\frac{\partial C}{\partial x}\right)$$

D is the mass diffusivity of solids. Integrating with respect to x , and designating the transmembrane flux, $MV/Mt = J$, and using the boundary conditions: $C = C_4$ at $x = \delta$:

$$\ln\left(\frac{C}{C_\infty}\right) = \frac{J}{D}(\delta - x) \quad (13.23)$$

At the surface, $x = 0$ and $C = C_s$.

$$\ln\left(\frac{C_s}{C_\infty}\right) = \frac{J}{D}\delta \quad (13.24)$$

Equation (13.24) shows that polarization concentration expressed as the ratio of surface to bulk solids concentration increases as the transmembrane flux and thickness of boundary layer increases. Equation (13.24) demonstrates that polarization concentration can be reduced by reducing transmembrane flux and decreasing the boundary layer thickness. Since flux must be maximized in any filtration, reduced polarization concentration can be achieved at maximum flux if high fluid velocities can be maintained on the membrane surface to decrease the boundary layer thickness, δ .

Rearranging Equation (13.24):

$$J = \frac{D}{\delta} \ln\left(\frac{C_s}{C_\infty}\right)$$

The ratio D/δ may be represented by a mass transfer coefficient for the solids, k_s . Thus:

$$J = k_s[\ln(C_s) - \ln(C_4)] \quad (13.25)$$

Equation (13.25) shows that a semi-log plot of the bulk concentration C_4 against the transmembrane flux under conditions where C_s is constant, will be linear with a negative slope of $1/k_s$. Thus, flux will

be decreasing with increasing bulk solids concentration and the rate of flux decrease will be inversely proportional to the mass transfer coefficient for solids transport between the surface and the fluid bulk.

Equations for estimation of mass transfer coefficients have been applied to determine the effects of cross-flow velocity on transmembrane flux, when polarization concentration alone controls flux. In Chapter 12, mass transfer coefficients were determined using the same equations as for heat transfer. The Sherwood number (Sh) corresponds to the Nusselt number; and the Schmidt number (Sc) corresponds to the Prandtl number.

The Dittus-Boelter equation can thus be used for estimation of mass transfer in turbulent flow.

$$\text{Sh} = 0.023 \text{Re}^{0.8} \text{Sc}^{0.33}$$

Because $\text{Sh} = k_s d_h / D$; $\text{Re} = d_h v \rho / \Phi$; and $\text{Sc} = \Phi / (D \cdot \rho)$:

$$k_s = 0.023 \frac{D}{d_h} \frac{d_h^{0.8} v^{0.8} \rho^{0.8}}{\mu^{0.8}} \frac{\mu^{0.33}}{D^{0.33} \rho^{0.33}} = \frac{0.023 D^{0.67} v^{0.8} \rho^{0.47}}{d_h^{0.2} \mu^{0.47}} \quad (13.26)$$

Although the Dittus-Boelter equation has been derived for tube flow, an analogy with pressure drops through non-circular conduits will reveal that equations for tube flow can be applied to noncircular conduits if the hydraulic radius is substituted for the diameter of the tube. D = mass diffusivity, m^2/s ; d_h = hydraulic radius = 4 (cross-sectional area)/wetted perimeter.

If fluid flows in a thin channel between parallel plates with width W and channel depth, $2b$:

$$d_h = 4(2b)(W)/(4b + 4W) = 2bW/(b + w)$$

If $b \ll W$, $d_h = 2b$ = the channel depth.

In laminar flow, the Sieder-Tate equation for heat transfer can be used as an analog to mass transfer:

$$\text{Sh} = 1.86 [\text{Re} \cdot \text{Pr} \cdot (d/L)]^{0.33} \quad (13.27)$$

Substituting the expressions for Sh, Re, and Pr:

$$k_s = 1.86 \frac{v^{0.33} D^{0.66}}{d_h^{0.33} L^{0.33}} \quad (13.28)$$

L is the length of the channel.

Equations (13.25) and (13.28) can be used to predict transmembrane flux when polarization concentration occurs if the diffusivity D of the molecular species involved and the surface concentration are known. The form of these equations agrees with experimental data. However it is ineffective in predicting actual transmembrane flux by the inability to predict the concentration at the membrane surface, C_s . The value of these equations is in interpolating within experimentally observed values for flux, and in extrapolating within reasonable limits, fluxes when data at one set of operating conditions are known. Porter (1979) suggests using the Einstein-Stokes equation (equation. 29) to estimate D :

$$D = \frac{1.38 \times 10^{-23} T}{6\pi\mu r} \quad (13.29)$$

where D is in m^2/s , $T = \text{K}$, Φ = medium viscosity in $\text{Pa} \cdot \text{s}$, and r = molecular radius in meters.

Example 13.5. The molecular diameter of β -lactoglobulin having a molecular weight of 37,000 daltons is $1.2 \times 10^{-9} \text{m}$. When performing ultrafiltrations at 30°C at a membrane surface velocity of 1.25 m/s , solids concentration in the feed of 12% and transmembrane pressure of 414 kPa, the flux was $6.792 \text{ L}/(\text{m}^2 \cdot \text{h})$. Calculate the concentration at the membrane surface, and the flux under the

same conditions but at a higher cross-membrane velocity of 2.19 m/s. The membrane system was a thin channel with a separation of 7.6 mm. Flow path was 30 cm long. The viscosity of the solution at 30°C was 4.8 centipoise, and the density was 1002 kg/m³.

Solution:

The diffusivity using Equation (13.29) is

$$D = \frac{1.38 \times 10^{-23}(30 + 273)}{6\pi(4.8)(0.001)(1.2 \times 10^{-9})} = 3.851 \times 10^{-11} \text{ m}^2/\text{s}$$

The hydraulic radius, d_h = channel depth = 7.6×10^{-3} m. The Reynolds number is

$$\text{Re} = 7.6 \times 10^{-3}(1.25)(1002)/[(4.8)(0.001)] = 1983$$

For turbulent flow, (Eq. 13.26):

$$\begin{aligned} k_s &= \frac{0.023(3.851 \times 10^{-11})^{0.66}(1.25)^{0.33}(1002)^{0.47}}{(7.6 \times 10^{-3})^{0.2}[(4.8)(0.001)]^{0.47}} = \frac{0.023(1.338 \times 10^{-7})(1.076)(25.72)}{0.376(0.081317)} \\ &= 2.785 \times 10^{-6} \text{ m/s} \end{aligned}$$

Given: $J = 6.792 \text{ L}/(\text{m}^2 \cdot \text{h}) = 1.887 \times 10^{-6} \text{ m}^3/\text{m}^2 \cdot \text{s}$

Using Equation (13.25): $C_s = C_4[e]^{J/k_s}$

C_4 is given as 0.12 g solids/g soln.

$$C_s = 0.12[e]^{1.88 \times 10^{-6}/2.785 \times 10^{-6}} = 0.12(1.969) = 0.236 \text{ g solute/g soln.}$$

For $v = 2.19 \text{ m/s}$:

$$k_s = 2.785 \times 10^{-6} \left[\frac{2.19}{1.25} \right]^{0.8} = 4.362 \times 10^{-6} \text{ m/s}$$

Using Equation (13.25):

$$J = 4.362 \times 10^{-6} [\ln(0.236/0.12)] = 2.95 \times 10^{-6} \text{ m}^3/(\text{m}^2 \cdot \text{s}) \text{ or } 10.62 \text{ L}/(\text{m}^2 \cdot \text{h})$$

13.1.10 Solute Rejection

Solute rejection in membrane separations is dependent on the type of membrane and the operating conditions. A solute rejection factor, R , is used, defined as:

$$R = \frac{C_s - C_p}{C_s} \quad (13.30)$$

where C_s = concentration of solute on the membrane surface on the retentate side of the membrane, and C_p = concentration of solute in the permeate.

Equation (13.30) shows that polarization concentration and increasing solute concentration in the feed, decreases the solute rejection by membranes.

Rejection properties of membranes are specified by the manufacturer in terms of the “molecular weight cut-off,” an approximate molecular size that will be retained by the membrane with a rejection

factor of 0.99 in very dilute solutions. The ideal membrane with a sharp molecular weight cut-off does not exist. On a particular membrane, the curve for rejection factor against molecular weight is often sigmoidal with increasing molecular weight of solute. Low molecular weight solutes will completely pass through the membrane and $R = 0$. As the solute molecular weight increases, small increases in R will be observed until the molecular size reaches that which will not pass through a majority of the pores. When the molecular size exceeds the size of all the pores, the rejection factor will be 1.0. The pore size distribution therefore, determines the distribution of molecular sizes which will be retained by the membrane. Some solutes will be retained because they are repelled by the membrane at the surface. This is the case with mineral salts on cellulose acetate membrane surfaces. This property of a membrane to repel a particular solute will be beneficial under conditions where separation from the solvent is desired (e.g., concentration) because high rejection factors can be achieved with larger membrane pore size therefore allowing solute rejection at high transmembrane flux.

Interactions between solutes also affect the rejection factor. For example, rejection factor for calcium in milk or whey is higher than aqueous calcium solutions. A protein to calcium complex will bind the calcium preventing its permeation through the membrane.

13.1.11 Sterilizing Filtrations

Sterilizing filtrations employ either depth cartridge filters or microporous membrane filters in a plate and frame or cartridge configuration. These filtrations are MF processes. Microporous membrane filters have pore sizes smaller than the smallest particle to be removed and performs a sieving process. They are preferred for sterilizing filtrations on liquid because the pressure drop across the membrane is much smaller than in a depth filter and the possibility of microorganisms breaking through is minimal. Pore size of microporous membranes for sterilizing filtrations is less than $0.2 \mu\text{m}$.

The filtration rate in sterilizing filtrations has been found by Peleg and Brown (J. Food Sci. 41:805, 1976) to follow the following relationship:

$$\frac{dV}{dt} = k \frac{V^{-n}}{c} \quad (13.31)$$

where c is load of microorganisms and suspended material that is removed by the filter, and k and n are constants which are characteristic of the fluid being filtered, the filter medium, the suspended solids, and fluid velocity across the membrane surface. k is also dependent on the transmembrane pressure. n is greater than 1; therefore, filtration rate decreases rapidly with increase in filtrate volume. No cake accumulation occurs in this type of filtration. The time for membrane replacement and pre-sterilization must be included in the analysis of the optimum cycle time and procedures for optimization will be similar to that in the section "Optimization of Filtration Cycles."

Cycle time can be increased when fluid is in cross-flow across the membrane surface at high velocities. This configuration minimizes solids deposition and membrane fouling. Fouled membrane surfaces may be rejuvenated by occasionally interrupting filtration through reduction of transmembrane pressure while maintaining the same velocity of fluid flow across the membrane. This procedure is called "flushing," as opposed to "backwashing" where the transmembrane pressure is reversed. Some membrane configurations are suitable for backwashing, while membrane fragility may restrict removal of surface deposits by flushing in other configurations. When rejuvenation is done by flushing or backflushing, the flushing fluid must be discarded or filtered through another coarser filter to

remove the solids, otherwise, mixing with new incoming feed will result in rapid loss of filtration rate.

Pre-sterilization of filter assemblies may be done using high pressure steam, or using chemical sterilants such as hydrogen peroxide, iodophores, or chlorine solutions. Care must be taken to test for filter integrity after pre-sterilization, particularly when heating of filter assemblies is used for presterilization. One method to test for filter integrity in line, is the “bubble point test,” where the membrane is wetted, sterile air is introduced, and the pressure needed to dislodge the liquid from the membrane is noted. Intact membranes require specific pressures to dislodge the liquid from the surface and any reduction in this bubble pressure is an indication of a break in the membrane.

Sterilizing filtrations are successfully employed in cold pasteurization of beer and wine, in the pharmaceutical industry for sterilization of injectable solutions, and in the biotechnological industry for sterilization of fermentation media and enzyme solutions.

Example 13.6. Data on flux during membrane filtration to clarify apple juice (Mondor et al. Food Res. International 33:539–548, 2000) showed the flux to follow two different domains when plotted with time. The initial rapid flux decay was attributed to deposition of solids on the membrane pores, and the domain where flux appear to level off with time was attributed to be due to concentration polarization and formation of a gel layer by the deposited solids on the membrane surface. If J_0 is the flux rate at time = 0, J_{41} is the flux corresponding to the point where flux levels off in the first part of the filtration curve, and J_{42} is the flux corresponding to the time when flux leveled off in the second part of the filtration curve, then the flux over the whole filtration cycle can be expressed as:

$$J = (J_0 - J_{\infty 1}) \exp(-\alpha t) + (J_{\infty 1} - J_{\infty 2}) \exp(-\beta t) + J_{\infty 2}$$

An experiment involving cross-flow filtration of apple juice through a PVDF membrane system with a pore size of 0.2 micrometers and a total membrane surface area of 1.0 m². Cross flow velocity was 3 m/s and transmembrane pressure was 1.5 Bars. The apple juice was obtained by pressing pectinase enzyme treated ground apples with rice hulls as filtration aid through multiple layers of cheese cloth in a bladder press. The data (time in hours, flux in liters/m² h) are as follows: (0.11, 32), (0.24, 28.6), (0.55, 22.7), (0.96, 18.1), (1.2, 15.1), (2.5, 9.8), (5.3, 5.9), (7.4, 4.7), (8, 4.7), (9, 4.6).

(a) Assuming that a cleaned membrane will result in the same pattern of flux decay, how long would it take to recover 15 L of the clarified juice (permeate)?

Solution:

The first term in the flux decay equation above is good for $t = 0$ to $t = t_{s1}$ where t_{s1} corresponds to the end of the first stage of the filtration cycle. This time is determined by plotting $\ln(J - J_{42})$ against time to see where the linear portion deviates from the experimental data curve. A regression is then conducted for the range of time where the curve is linear. The second term in the above expression for J represents the flux decay from the start of the second stage in the filtration cycle. Again, the linear portion of the $\ln(J - J_{42})$ versus time curve is located and a linear regression is conducted to obtain the slope. The time variable in the second term should be the difference between the actual time and the start of the linear plot close to the actual experimental curve.

J_{42} from the above data = 4.6 L/m²h.

The transformed data is as follows:

Time (h)	J (L/m ² h)	$\ln(J + J_{42})$
0.11	32	3.31
0.24	28.6	3.18
0.55	22.7	2.89
0.96	18.1	2.60
1.2	15.1	2.35
2.5	9.8	1.65
5.3	5.9	0.26
7	4.7	-2.3
8	4.7	-2.3

The first linear segment fitted $t = 0.11$ to $t = 2.5$. This segment has a slope of -0.69 and an intercept of 3.31 . The value of $J_{41} = 4.7$ L/m²h. The second line segment fitted the curve from $t = 5.3$ to 8 and has a slope of -1.0 . This line segment intersects the first line segment at $t = 3.5$. Thus the equation for J is as follows: $J = (32 - 4.7) \exp(-0.69 \cdot t) + (4.7 - 4.6) \exp(-1.0(t - 3.5)) + 4.6$
 $J = 27.3 \exp(-0.69 \cdot t) + 0.1 \exp(-(t - 3.5)) + 4.6$. V = volume of permeate.

$$V = \int_0^t J dt = \int_0^t \{27.3[e]^{-0.69t} + 0.1[e]^{-(t-3.5)} + 4.6\}$$

$$V = \frac{-27.3}{0.69} [e]^{-0.69t} - 0.1[e]^{-(t-3.5)} + 4.6t$$

This equation will be solved using Excel.

Set up volume increments in 0.1 hours. Suppose $t = 0.1$ h is in $a3$. The value of the integral will be: $(-27.3/0.69) \cdot \exp(-0.79 \cdot a3) - 0.1 \cdot \exp(-(a3 - 3.5)) + 4.6 \cdot a3 + (27.3/0.69) + 0.1$. The calculated values are as follows:

$t = 0$, $V = 0$; $t = 0.1$, $V = 0.20$; $t = 0.3$, $V = 6.42$, $t = 0.4$, $V = 0.3$, $t = 0.5$, $V = 11.9$; $t = 0.6$, $V = 14.5$, $t = 0.7$, $V = 16.8$. Thus, it would take 0.62 hours of filtration to obtain 15 L of filtrate.

13.1.12 Ultrafiltration

Ultrafiltration is widely employed in the increasingly important biotechnological industry for separation of fermentation products, particularly enzymes. Its largest commercial use is in the dairy industry for recovery of proteins from cheese whey and for pre-concentration of milk for cheese making. UF systems also have potential for use as biochemical reactors, particularly in enzyme or microbial conversion processes where the reaction products have an inhibitory effect on the reaction rate.

A large potential use for UF is in the extraction of nectar from fruits which cannot be pressed for extraction of the juice. The fruit mash is treated with pectinase enzymes and the slurry is clarified by UF. UF applications in recycling of food processing waste water, and in recovery of valuable components of food processing wastes are currently in the developmental stages. More membranes for UF applications are available than for RO applications, indicating increasing commercial applications for UF in the food industry.

13.1.13 Reverse Osmosis

Reverse osmosis has potential for generating energy savings in the food processing industry, when used as an alternative to evaporation in the concentration of products containing low molecular weight solutes. The early work on RO has been devoted to desalination of brackish water, and a number of RO systems have now been developed which can purify waste water for re-use after an RO treatment. In the food industry, RO has potential for juice concentration without the need for application of heat.

In RO, the transmembrane pressure is reduced as a driving force for solvent flux by the osmotic pressure. Since solutes separated by RO have low molecular weights, the influence of concentration on osmotic pressure is significant. Equation (12.5) in Chapter 12 can be used for determining the osmotic pressure. Because the product of the activity coefficient of water and the mole fraction of water is the water activity, this equation can be written as:

$$\pi = -\frac{RT}{V} \ln(a_w) \quad (13.32)$$

where π = osmotic pressure, R = gas constant, T = absolute temperature, and V = molar volume of water. a_w = water activity.

The minimum pressure differential needed to force solvent across a membrane in RO is the osmotic pressure. Equations (12.17) and (12.21) in Chapter 12 can be used to determine a_w of sugar solutions.

Example 13.7. Calculate the minimum transmembrane pressure that must be used to concentrate sucrose solution to 50% sucrose at 25°C.

Solution:

From the Example 12.1 in Chapter 12, the water activity of a 50% sucrose solution was calculated to be 0.935.

$R = 8315 \text{ N m / (kgmole} \cdot \text{K)}$; $T = 303 \text{ K}$, and the density of water at 25°C = 997.067 kg/m³ from the steam tables.

$$V = \frac{18 \text{ kg}}{\text{kgmole}} \frac{1}{997.067 \text{ kg/m}^3} = 0.018053 \text{ m}^3/\text{kgmole}$$

$$\begin{aligned} \pi &= \frac{-[8315 \text{ Nm / (kgmole} \cdot \text{K)}][303 \text{ K}]}{0.018053 \text{ m}^3/\text{kgmole}} \ln(0.935) \\ &= 9379 \text{ kPa} \end{aligned}$$

A minimum of 9379 kPa transmembrane pressure must be applied just to overcome the osmotic pressure of a 50% sucrose solution.

This example illustrates the difficulty in producing very high concentrations of solutes in reverse osmosis processes, and the large influence of concentration polarization in reducing transmembrane flux in RO systems.

Transmembrane flux in RO systems is proportional to the difference between the transmembrane pressure and the osmotic pressure.

$$J = \left(\frac{k_w}{x} \right) (P - \Delta\pi) \quad (13.33)$$



Figure 13.8 Visual BASIC program for problem involving reverse osmosis concentration of orange juice.

where J = transmembrane flux, kg water/(s · m²); k_w = mass transfer coefficient, s; x = thickness of membrane, m; P = transmembrane pressure, Pa; and π = osmotic pressure, Pa.

Example 13.8. The pure water permeability of cellulose acetate membrane having a rejection factor of 0.93 for a mixture of 50% sucrose and 50% glucose is 34.08 kg/h of water at a transmembrane pressure of 10.2 atm (1034 kPa) for a membrane area of 0.26 m². This membrane system had a permeation

rate of 23.86 kg/h when 1% glucose solution was passed through the system at a transmembrane pressure of 10.2 atm. at 25°C.

Orange juice is to be concentrated using this membrane system. In order to prevent fouling, the orange juice was first centrifuged to remove the insoluble solids, and only the serum which contained 12% soluble solids was passed through the RO system. After centrifugation, the serum was 70% of the total mass of the juice.

Assume that the soluble solids are 50% sucrose and 50% glucose. The pump that feeds the serum through the system operates at a flow rate of 0.0612 kg/s (60 mL/s of juice having a density of 1.02 g/mL). The transmembrane pressure was 2758 kPa (27.2 atm).

Calculate the concentration of soluble solids in the retentate after one pass of the serum through the membrane system.

Solution:

This problem illustrates the effects of transmembrane pressure, polarization concentration and osmotic pressure on transmembrane flux and solute rejection in reverse osmosis systems. The governing equations are Equation (13.25) for polarization concentration and Equation (13.33) for transmembrane pressure.

The reduction in the pure water permeability when glucose solution is passed through the membrane system can be attributed to polarization concentration. Equation (13.25):

$J = k_s \ln (C_s/C_4)$. Let N_w = water permeation rate in kg/h.

$N_w = JA \text{ m}^3/\text{s} (3600\text{s/h})(1000\text{kg/m}^3)$.

$$J = \left(\frac{N_w}{A} \right) \left(\frac{1}{3.6} \right) \times 10^{-6}$$

The osmotic pressure at the membrane surface responsible for the reduction of transmembrane flux in the 1% glucose solution is calculated using Equation (13.33).

$$N_w = \left(k_w \frac{A}{x} \right) (P - \pi)$$

The factor $(k_w A/x)$ can be calculated using the pure water permeability data, where $\pi = 0$:

$$\left(k_w \frac{A}{x} \right) = \frac{N_w}{P} = \frac{34.08}{10.2} = 3.34 \text{ kg}/(\text{h} \cdot \text{atm})$$

For the 1% glucose solution, using Equation (13.33):

$$N_w = \left(k_w \frac{A}{x} \right) (P - \pi)$$

$$23.86 = 3.34(10.2 - \pi)$$

$$\pi = 3.05 \text{ atm.}$$

A 1% glucose solution has a water activity of practically 1.0, therefore, the osmotic pressure must be exerted at the membrane surface. Thus, C_s can be calculated as the glucose concentration that gives an osmotic pressure of 3.05 atm. Using Equation (13.32), for $P = 3.05(101,325) = 309,041 \text{ Pa.}$:

$$309,041 = -(8315)(298/0.018) \ln (a_w)$$

$$a_w = e^{-0.00225} = 0.99775$$

For very dilute solutions, $a_w = x_w$. Let C_s = solute concentration at the surface, g solute/g solution.

$$a_w = x_w = \frac{(1 - C_s)/18}{(1 - C_s)/18 - C_s/180}$$

$$a_w = \frac{(1 - C_s)(18)(180)}{18[180(1 - C_s) + 18C_s]} = 0.99775$$

$$321.271C_s + 3232.71 - 3232.71C_s = 3420 - 3420C_s$$

$$C_s = 7.29/330.561 = 0.022 \text{ g solute / g solution}$$

Solving for J from the permeation rate:

$$J = (23.86/0.26)(1/3.6) \times 10^{-6} = 2.55 \times 10^{-5} \text{ m/s}$$

Using Equation (13.25):

$$k_s = 2.55 \times 10^{-5} / \ln(0.022/0.01) = 3.234 \times 10^{-5} \text{ m/s}$$

For the orange juice serum: $C_4 = 0.12$ g solute/g soln. Solving for C_s using Equation (13.25):

$$J = 3.234 \times 10^{-5} \ln(C_s/0.12)$$

Solving for N_w from J:

$$N_w = J A (3.6)(10^6) = [3.234 \times 10^{-5} \ln(C_s/0.12)](0.26)(3.6 \times 10^6) = 30.27 \ln(C_s/0.12)$$

Solving for N_w from the transmembrane pressure using Equation (13.36):

$$N_w = (k_w A/x)(P - \pi) = 3.34(27.2 - \pi)$$

Equating the two equations for permeation rate:

$$30.27 \ln(C_s/0.12) = 3.34(27.2 - \pi)$$

$$\ln(C_s/0.12) = 0.1103(27.2 - \pi)$$

Solving for π in atm using Equation (13.32):

$$\pi = -(8315)(298/0.018) \ln(a_w) [1 \text{ atm}/101,325 \text{ Pa}] = -1358.59 \ln(a_w), \text{ atm}$$

Substituting in the equation for C_s :

$$\ln(C_s/0.12) = 0.1103[27.2 + 1358.59 \ln(a_w)]$$

a_w can be solved in terms of C_s as follows:

For sucrose: x_{ws} = mole fraction of water in the sucrose fraction of the solution; a_{ws} = water activity due to the sucrose fraction.

$$x_{ws} = \frac{(1 - 0.5C_s)/18}{(1 - 0.5C_s)/18 + 0.5C_s/342}$$

$$a_{ws} = x_{ws}[10]^{-2.7(1-x_{ws})^2}$$

For the glucose fraction of the mixture: Let x_{wg} = mole fraction of glucose; a_{wg} = water activity due to the glucose fraction.

$$x_{wg} = \frac{(1 - 0.5C_s)/18}{(1 - 0.5C_s)/18 + 0.5C_s/180}$$

$$a_{wg} = x_{wg}[10]^{-0.7(1-x_{wg})^2}$$

$$a_w = a_{ws} \cdot a_{wg}$$

C_s will be solved using a Visual BASIC program. In this program, a wide range of values of C_s from 0.1 to 0.2 was first substituted with a larger step change of 0.01. The printout was then checked for the two values of C_s between which the function F crossed zero. A narrow range of C_s between 0.115 and 0.125 was later chosen with a narrower step change in order to obtain a value of C_s to the nearest third decimal place which satisfied the value of the function F to be zero.

The value of C_s will be 0.1949. The rejection factor will be used to calculate the permeate solute concentration.

$$R = (C_s - C_p)/C_s$$

$$C_p = C_s(1 - R) = 0.1949(1 - 0.93)$$

$$C_p = 0.0136 \text{ g solute/g permeate.}$$

Total mass balance:

$$F = P + R; F = 0.0612 \text{ kg/s (3600s/h)} = 220.3 \text{ kg/h}$$

$$P = N_w/(1 - C_p)$$

$$N_w = 30.27 \ln(0.1949/0.12) = 14.68 \text{ kg/h}$$

$$P = 14.68/(1 - 0.0134) = 14.87 \text{ kg/h}$$

$$R = 220.3 - 14.87 = 205.43 \text{ kg/h}$$

Solute balance: $FC_f = RC_r + PC_p$

$$0.12(220.3) = 205.43(C_r) + 14.87(0.0134)$$

$$C_r = 0.128 \text{ g solute/g retentate}$$

The effect of polarization concentration shown in this example problem demonstrates that increasing transmembrane pressure may not always result in a higher flux. A pressure will be reached beyond which polarization concentration will negate the effect of the applied pressure and any further increase in transmembrane pressure will result in no further increase in flux.

Fouling remains a major problem in both RO and UF applications. Optimization of operating cycles using the principles discussed in the section "Optimization of Filtration Cycles" is an aspect of the operation to which an engineer can make contributions to successful operations. Application of theories and equations on polarization concentration as discussed in the preceding sections will help in identifying optimum operating conditions, but absolute values of transmembrane flux are better obtained empirically on small systems and results used for scale-up than calculating theoretical values. Material balance calculations as discussed in Chapter 3 in the section "Multistage Processes," Example 3.21, will also help in analyzing UF systems, particularly in relation to recycling and multi-stage operations to obtain the desired composition in the retentate.

13.1.14 Temperature Dependence of Membrane Permeation Rates

Temperature affects liquid permeation rates through membranes in proportion to the change in viscosity of the fluid with temperature. If the solvent is water, and permeate flux at one temperature is given, the permeation rate at any other temperature can be calculated by:

$$J_{T1} = J_{T2} \frac{\mu_{T2}}{\mu_{T1}}$$

where J_{T1} and J_{T2} are fluxes at $T1$ and $T2$ respectively. The viscosity of water at temperature T in Celsius is

$$\mu = \frac{1795 \cdot 10^{-6}}{1 + 0.036T + 0.000185T^2}$$

where μ = viscosity in Pa s and T is temperature in °C.

13.1.15 Other Membrane Separation Processes

Membranes are also used to remove inorganic salts from protein solutions, or for recovery of valuable inorganic compounds from process wastes. Dialysis and electrodialysis are two commonly used processes.

Dialysis is a diffusion rather than pressure-driven process. A solute concentration gradient drives solute transport across the membrane. Dialysis is well-known in the medical area, for removing body wastes from the blood of persons with diseased kidneys. In the food and biochemical industries, dialysis is used extensively for removal of mineral salts from a protein solution by immersing the protein solution contained in a dialysis bag or tube in flowing water. Solute flux in dialysis is very slow.

Electrodialysis is a process where solute migration across the membrane is accelerated by the application of an electromotive potential. Anion and cation selective membranes are used. The electromotive potential forces the migration of ionic species across the membrane towards the appropriate electrode. Electro dialysis is used to demineralize whey, but food industry applications of the process are still rather limited.

13.2 SIEVING

Sieving is a mechanical size separation process. It is widely used in the food industry for separating fines from larger particles, and also for removing large solid particles from liquid streams prior to further treatment or disposal. Sieving is a gravity driven process. Usually a stack of sieves are used when fractions of various sizes are to be produced from a mixture of particle sizes.

To assist in the sifting of solids in a stack of sieves, sieve shakers are used. The shakers may be in the form of an eccentric drive that gives the screens a gyratory or oscillating motion, or it may take the form of a vibrator which gives the screens small amplitude high frequency up and down motion. When the sieves are inclined, the particles retained on a screen fall off at the lower end and are collected by a conveyor. Screening and particle size separation can thus be carried out automatically.

13.2.1 Standard Sieve Sizes

Sieves may be designated by the opening size, US-Sieve mesh or Tyler Sieve mesh. The Tyler mesh designations refer to the number of openings per inch, while the US-Sieve mesh designations is the metric equivalent. The latter has been adopted by the International Standards Organization. The two mesh designations have equivalent opening size although the sieve number designations are not exactly the same. Current sieve designations, unless specified, refer to the US-Sieve series. Size of particles are usually designated by the mesh size that retains particles that have passed through the next larger screen size. A clearer specification of particle size by mesh number would be to indicate by a plus sign before the mesh size that retains the particles and by a negative sign the mesh size that passed the particles. If a mixture of different sized particles are present, the designated particle size must be the weighted average of the particle sizes.

Table 13.5 shows US sieve mesh designations and the size of openings on the screen. A cumulative size distribution of powders can be made by sieving through a series of standard sieves and determining the mass fraction of particles retained on each screen. The particles are assumed to be spherical with a diameter equal to the mean of the sieve opening which passed the particles and that which retained the particles.

Example 13.9. Table 13.6 shows the mass fraction of a sample of milled corn retained on each of a series of sieves. Calculate a mean particle diameter which should be specified for this mixture.

Solution:

The sieve opening is obtained from Table 13.6. The mean particle size retained on each screen is the mean opening size between the screens which retained the particular fraction and the one above

Table 13.5 Standard US-Sieve Sizes.

US-Sieve Size (mesh)	Opening (mm)	US-Sieve Size (mesh)	Opening (mm)
2.5	8.00	35	0.500
3	6.73	40	0.420
3.5	5.66	45	0.354
4	4.76	50	0.297
5	4.00	60	0.250
6	3.36	70	0.210
7	2.83	80	0.177
8	2.38	100	0.149
10	2.00	120	0.125
12	1.68	140	0.105
14	1.41	170	0.088
16	1.19	200	0.074
18	1.00	230	0.063
20	0.841	270	0.053
25	0.707	325	0.044
30	0.595	400	0.037

Source: Perry, R. H., Chilton, C. H., and Kirkpatrick, S. D. 1963. *Chemical Engineers Handbook*, 4th ed. McGraw-Hill Book Co., New York.

Table 13.6 US-Sieve Size Distribution of Power Sample and Calculation of Mean Particle Diameter.

<i>Mass Fraction Retained</i>	<i>US-Sieve Screen</i>	<i>Sieve Opening (mm)</i>	<i>Particle size</i>	<i>Fraction × Size</i>
0	35	0.500		
0.15	45	0.354	0.437	0.065
0.35	60	0.250	0.302	0.1057
0.45	80	0.177	0.213	0.095585
0.05	120	0.125	0.151	0.00755
				Sum = 0.2741

it. The mass fraction is multiplied by the mean particle size on each screen and the sum will be the weighted mean diameter of the particle. From Table 13.5, the mean particle diameter is 0.2741 mm.

This example clearly shows that the choice of sieves used in classifying the sample into the different size fractions, will affect the mean particle diameter calculated. The use of a series of sieves of adjacent sizes in Table 13.5 is recommended.

13.3 GRAVITY SEPARATIONS

This type of separation depends on density differences between several solids in suspension or between the suspending medium and the suspended material. Generally, the force of gravity is the only driving force for the separation. However, the same principles will apply when the driving force is increased by application of centrifugal force.

13.3.1 Force Balance on Particles Suspended in a Fluid

When a solid is in suspension, an *external force*, F_e , acts on it to move in the direction of the force. This external force may be gravitational force, in which case it will cause a particle to move downward, or it can be centrifugal force, which will cause movement toward the center of rotation. In addition, a *buoyant force*, F_b , exists that acts in a direction opposite the external force. Another force, the *drag force*, F_d , also exists, and this force is due to motion of the suspended solid and acts in the direction opposite the direction of flow of the solid. Let F_t = the net force on the particle. The component of forces in the direction of solid motion will obey the following force balance equation.

$$F_t = F_e - F_d - F_b \quad (13.34)$$

In applying Equation (13.34), the sign on F_t will determine its direction based on the designation of the direction of F_e as the positive direction.

13.3.1.1 Buoyant Force

F_b is the mass of fluid displaced by the solid multiplied by the acceleration provided by the external force. Let a_e = acceleration due to the external force, m = mass of particle, ρ_p = density of particle, ρ = density of the fluid.

The mass of displaced fluid = volume of the particle /density = m/ρ_p

$$F_b = m a_c \left(\frac{\rho}{\rho_p} \right) \quad (13.35)$$

The mass of displaced fluid = $m(\rho/\rho_p)$.

13.3.1.2 Drag Force

F_d is fluid resistance to particle movement. Dimensional analysis will be used to derive an expression for F_d .

Assume that the F_d/A_p , where A_p is the projected area perpendicular to the direction of flow; F_d is a function of the particle diameter, d ; v_r is the relative velocity between fluid and particle; ρ is the fluid density; ρ and μ is the fluid viscosity.

The general expression used in dimensional analysis is that the functionality is a constant multiplied by the product of the variables each raised to a power.

$$\frac{F_d}{A_p} = C(v_r)^a \rho^b \mu^c d^e$$

Expressing in terms of the base units, mass, M, length, L, and time, t.

$$\frac{ML}{t^2} \frac{1}{L^2} = \frac{L^a}{t^a} \frac{M^b}{L^{3b}} \frac{M^c}{L^c t^c} L^e$$

Consider the coefficients of each base unit. To be dimensionally consistent, the exponents of each unit must the opposite side of the equation.

Exponents of L:

$$-1 = a - 3b - c - e \quad (i)$$

Exponents of t:

$$2 = a + c; \quad a = 2 - c \quad (ii)$$

Exponents of M:

$$1 = b + c; \quad b = 1 - c \quad (iii)$$

Combining equations (ii) and (iii) in (i)

$$\begin{aligned} -1 &= 2 - c - 3(1 - c) - c + e \\ e &= -c \end{aligned}$$

Thus, the expression for drag force becomes:

$$\frac{F_d}{A_p} = C V^{2-c} \rho^{1-c} \mu^c d^{-c}$$

Combining terms with the same exponent:

$$\frac{F_d}{A_p} = C \left[\frac{\mu}{dv_r \rho} \right]^n (v_r)^2 \rho \quad (13.36)$$

The first two terms on the right are replaced by a drag coefficient, C_d , defined as $C_d = C/Re^n$.

Equation (13.36) is often written in terms of C_d as follows:

$$F_d = C_d \frac{(v_r)^2 \rho}{2} \quad (13.37)$$

Consider a spherical particle settling within a suspending fluid. A sphere has a projected area of a circle; $A_p = \pi d^2/4$. If particle motion through the fluid results in laminar flow at the fluid surface with the particle, $C_d = 24/Re$. The equation for drag force becomes:

$$F_d = \left(\frac{24}{Re} \right) \left(\frac{\pi d^2}{4} \right) (v_r)^2 \rho = 3\pi\mu d v_r \quad (13.38)$$

13.3.2 Terminal Velocity

The terminal velocity of the particle is the velocity when $dv_r/dt = 0$, that is, settling will occur at a constant velocity. Substituting Equations (13.35) and (13.38) into Equation (13.34):

$$F_t = ma_e - ma_e \left(\frac{\rho}{\rho_p} \right) - 3\pi\mu d v_r$$

$F_t = ma_p = m(dv_r/dt)$. The mass of the particle is the product of the volume and the density. For a sphere: $m = \pi d^3 \rho_p / 6$. Thus, at the terminal velocity, v_t :

$$ma_e \left(1 - \frac{\rho}{\rho_p} \right) = 3\pi\mu v_t d$$

Substituting for m :

$$v_t = \frac{a_e(\rho_p - \rho)d^2}{18\mu} \quad (13.39)$$

Equation (13.39) is *Stokes' law* for velocity of particle settling within the suspending fluid. For gravity settling, $a_e = g$. For centrifugation, $a_e = \omega^2 r_c$, where r_c = radius of rotation and ω = the angular velocity of rotation.

13.3.3 The Drag Coefficient

C_d used in the derivation of Equation (13.39) is only good when v_r is small and laminar conditions exists at the fluid-particle interface. In general, C_d can be determined by calculating an index K as follows:

$$K = d \left[\frac{a_e \rho (\rho - \rho_p)}{\mu^2} \right]^{0.33} \quad (13.40)$$

Data by Lapple and Shepherd (Ind. Eng. Chem. 32:605, 1940) shows that the value of C_d can be

determined for different values of K as follows:

If $K > 0.33$, or $Re < 1.9$; $C_d = 24/Re$

If $1.3 < K < 44$ or $1.9 < Re < 500$; $C_d = 18.5/Re^{0.6}$

If $K > 44$ or $Re > 500$; $C_d = 0.44$

If the Reynolds number at the particle to fluid interface exceeds 1.9, Equation (13.35) and (13.37) are combined in Equation (13.34), and under conditions when the particle is at the terminal velocity:

$$ma_e \left[1 - \left(\frac{\rho}{\rho_p} \right) \right] = C_d A_p (v_r)^2 \frac{\rho}{2}$$

Substituting $A_p = \pi d^2/4$; and $m = \pi d^3 \rho_p/6$ and solving for v_r :

$$v_r = 1.155 \left[\frac{a_e d (\rho_p - \rho)}{\rho C_d} \right]^{0.5} \quad (13.41)$$

Example 13.10. In the processing of soybeans for oil extraction, hulls must be separated from the cotyledons in order that the soy meal eventually produced will have high value as feed or as a material for further precessing for food proteins. The whole soybeans are passed between a cracking roll which splits the cotyledons and produces a mixture of cotyledons and hulls. Figure 13.9 shows a system that can be used to separate hulls from the cotyledons by air classification. The projected diameters and the densities of cotyledons and hulls are 4.76 mm and 1003.2 kg/m³ and 6.35 and 550 kg/m³, respectively. The process is carried out at 20°C. Calculate the terminal velocity of hulls and cotyledons in air. The appropriate velocity through the aperture will be between these two calculated terminal velocities.

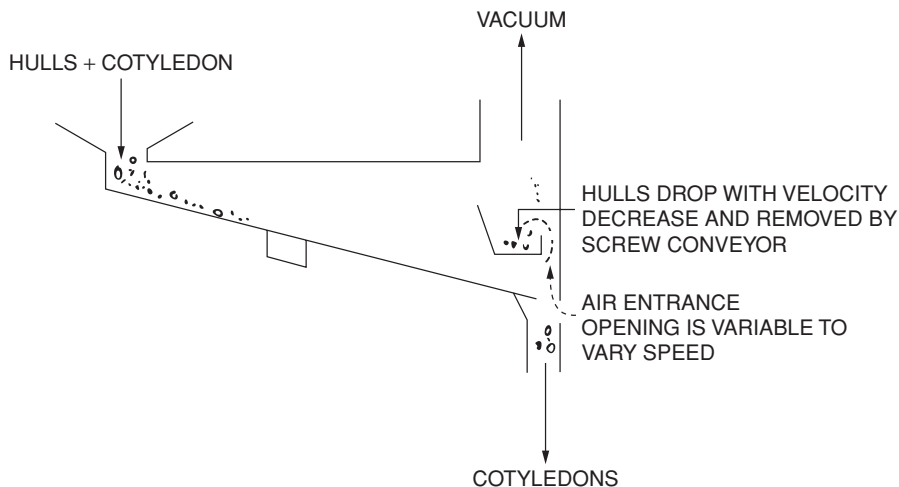


Figure 13.9 Diagram of air classification system to separate soybean hulls from the cotyledons.

Solution:

The density of air at 20°C is calculated using the ideal gas equation. The molecular weight of air is 29; atmospheric pressure = 101.325 kPa;

$$R = 8315 \text{ N} \cdot \text{M}/(\text{kgmole} \cdot \text{K})$$

$$\rho = \frac{p(29)}{RT} = \frac{101,325(29)}{8315(293)} = 1.206 \text{ kg/m}^3$$

The viscosity of air at 20°C is 0.0175 centipoise (from *Perry's Chemical Engineers Handbook*). Using Equation (13.40):

$$a_e = \text{acceleration due to gravity} = 9.8 \text{ m/s}^2.$$

For the cotyledons:

$$K = 0.00476 \left[\frac{9.8(1.206)(1003.2 - 1.206)}{[(0.0175)(0.001)]^2} \right]^{0.33} = 145$$

Because $K > 44$, $C_d = 0.44$.

Using Equation (13.41): $a_e = 9.8 \text{ m/s}^2$

$$v_r = 1.155 \left[\frac{9.8(0.00476)(1003.2 - 1.206)}{1.206(0.44)} \right]^{0.5} = 10.84 \text{ m/s}$$

For the hulls:

$$K = 0.00476 \left[\frac{9.8(1.206)(550 - 1.206)}{[0.0175(0.001)]^2} \right]^{0.33} = 118.9$$

$K > 444$; therefore, $C_d = 0.44$.

Using Equation (13.41):

$$v_r = 1.155 \left[\frac{9.8(0.00635)(550 - 1.206)}{1.206(0.44)} \right]^{0.5} = 9.266 \text{ m/s}$$

Thus air velocity between 9.266 and 10.84 m/s must be used on the system to properly separate the hulls from the cotyledons.

Equations (13.37) to (13.40) also applies in sedimentation, flotation, centrifugation, and fluidization of a bed of solids. In flotation separation where gravity is the only external force acting on the particles, Equation (13.39) shows that solids having different densities can be separated if the flotation fluid density is between the densities of the two solids. The solid with lower density will float and that with the higher density will sink. Air classification of solids with different densities as shown in the example can be achieved by suspending the solids in air of the appropriate velocity, the denser solid will fall and the lighter solid will be carried off by the air stream. Air classification is a commonly used method for removal of lighter foreign material from grains, and in fractionation of milled wheat into flour with different protein and bran contents. Density gradient separations are employed in fractionating beans of different degrees of maturity, and crab meat from scraps after manual removal of flesh.

In fluidization, the fluid velocity must equal the terminal velocity to maintain the particles in a stationary motion in the stream of air. Fluidized bed drying and freezing are commercially practiced in the food and pharmaceutical industries.

PROBLEMS

- 13.1. Based on data for apple juice filtration in Table 13.2, calculate the filtration area of a rotary filter that must be used to filter 4000 L/h of juice having a suspended solids content of 50 kg/m³. Assume k is proportional to solids content. The medium resistance increases with increasing pre-coat thickness. A 10-cm-thick precoat is usually used on rotary filters. Assume the medium resistance is proportional to the precoat thickness. The rotational speed of the filter is 2 rev/min and the diameter is 2.5 m. A filtration cycle on a rotary filter is the time of immersion of the drum in the slurry and in this particular system, 45% of the total circumference is immersed at any given time.
- 13.2. The following data were obtained in a laboratory filtration of apple juice using a mixture of rice hulls and perlite as the filter aid. The filtrate had a viscosity of 2.0 centipose. The suspended solids in the juice is 5 g/L, and rice hulls and perlite were added each at the same concentration as the suspended solids. The filter has an area of 34 cm². Calculate:
- The specific cake resistance and the medium resistance.
 - The optimum filtration time per cycle and the average volume of filtrate per unit area per hour at the optimum cycle time.

<i>Time(s)</i>	<i>Volume (mL)</i>	<i>Time (s)</i>	<i>Volume (mL)</i>
100	40	400	83
200	60	500	91
300	73		

- 13.3. The following data were reported by Slack [Process Biochem. 17(4):7, 1982] on flux rates at different solids content during ultrafiltration of milk. Test if the flux vs. solids content follow that might be predicted by the theory on polarization concentration. What might be the reasons for the deviation? All flow rates are the same and the same membrane was used in the series of tests.

<i>Mean solids Content (%)</i>	<i>Flux (L/(m² ⋅ h))</i>
12.3	28.9
13.6	25.5
14.9	22.1
24.1	23.8

- 13.4. The following analysis has been reported for retentate and permeate in ultrafiltration of skim milk. Retentate: 0.15% fat, 16.7% protein, 4.3% lactose, 22.9% total solids. Permeate: 0% fat, 0% protein, 4.6% lactose, 5.2% total solids.
- Calculate the rejection factor for lactose by the membrane used in this process.
 - If the membrane flux in this process follows the data in Problem 3, calculate the lactose content of skim milk which was subjected to a diafiltration process where the original milk containing 8.8% total solids, 4.5% lactose, 3.3% protein and 0.03% fat was concentrated to 17% total solids, diluted back to 10 % total solids and re-concentrated by UF to 20% total solids.

- 13.5. Calculate the average particle diameter and total particle surface area assuming spherical particles, per kg solids, for a powder which has a bulk density of 870 kg/m^3 and which has the following particle size distribution:

+14,	−10 mesh	10%
+18,	−14 mesh	14.6%
+25,	−18 mesh	22.3%
+35,	−45 mesh	30.2%
+60,	−45 mesh	22.9%

SUGGESTED READING

- Cheryan, M. 1986. Ultrafiltration Handbook. Technomic Publishing Co., Lancaster, PA.
- Crews, J. G. and Boddeker, K. W. 1994. Membrane Processes in Separation and Purification. Kluwer Academic Publishers, Boston.
- Green, D. W. and Mahoney, J. O. 1997. Perry's Chemical Engineers Handbook. 7th ed. Chapter 18 and 22. McGraw Hill, New York.
- Noble, R. D. and Stern, S. A. 1995. Membrane Separations Technology: Principles and Applications. Elsevier, New York.
- Poole J. B. and Doyle, D. 1968. Solid-Liquid Separation. Chemical Publishing Co., New York.
- Porter, M. C. 1979. Membrane Filtration. In: Handbook of Separation Techniques for Chemical Engineers. P. A. Schweitzer, Ed. McGraw-Hill, New York.
- Sourirajan, S. 1970. Reverse Osmosis. Logos Press, New York.